JOURNAL OF PROPULSION AND POWER
Vol. 18, No. 6, November–December 2002

Mass-Based Optimization of Thermal Management and Power Systems for Space Applications

K. D. Freudenberg,* W. E. Lear,† and S. A. Sherif‡
University of Florida, Gainesville, Florida 32611-6300
and
E. L. Golliher§
NASA John H. Glenn Research Center, Cleveland, Ohio 44135

Integration of new and existing technologies for thermal management will be required to meet the challenges associated with the increased need for an efficient, lightweight, heat-rejection system. Subsystem design requirements, such as thermal and mass management, must be brought into the design cycle to establish an optimal configuration. This paper provides a parametric analysis that determines the specific conditions under which a proposed system becomes advantageous from a weight-management standpoint. The analysis can be applied to essentially any space-operated thermally actuated heat pump providing power and/or refrigeration. By applying the techniques demonstrated in this paper, designers can identify and optimize conceptual configurations during the initial prototype development stages to reduce payload weight and increase financial savings. Examples of systems to which this analysis can be applied are presented and quantified.

Nomenclature

A	=	cross-sectional area, m^2
G_{sun}	=	local radiant solar heat flux [Equation (24)], W/m^2
m	=	mass, kg
$\tilde{m}$	=	system mass ratio (SMR)
Q'	=	heat-transfer rate, kW
T	=	temperature, °C
T^*	=	normalized temperature
w'	=	work rate, kW
α	=	normalized mass per area term
ε	=	emissivity
ζ	=	structural parameter
η	=	efficiency
λ	=	mass per unit area, kg/m^2
μ	=	turbomachinery mass fraction
ξ	=	percentage of Carnot efficiency
σ	=	Stephan–Boltzmann constant, 5.67×10^{-8} W/m^2-K^4

Subscripts

C	=	Carnot
col	=	collector
e	=	high-temperature reservoir source, refrigeration cycle
H	=	high-temperature reservoir source, power cycle
P	=	power
R	=	refrigeration
rad	=	radiator
rad,o	=	ideal passive radiator
rad,p	=	actual passive radiator
s	=	surrounding temperature reservoir source
sys	=	system, excluding collector and radiator
T	=	total
t,act	=	total actual system including collector and radiator

Received 4 October 2001; revision received 17 May 2002; accepted for publication 14 June 2002. Copyright © 2002 by the authors. Published by the American Institute of Aeronautics and Astronautics, Inc., with permission. Copies of this paper may be made for personal or internal use, on condition that the copier pay the $10.00 per-copy fee to the Copyright Clearance Center, Inc., 222 Rosewood Drive, Danvers, MA 01923; include the code 0748-4658/02 $10.00 in correspondence with the CCC.

*Research Assistant, Department of Mechanical and Aerospace Engineering, P.O. Box 116300.
†Associate Professor, Department of Mechanical and Aerospace Engineering, P.O. Box 116300. Associate Fellow AIAA.
‡Professor, Department of Mechanical and Aerospace Engineering, P.O. Box 116300. Associate Fellow AIAA.
§Electrical Engineer, Thermo-Mechanical Systems Branch, 21000 Brookpark Road, MS 301-2. Member AIAA.

Introduction

INCREASED interest in space exploration and the drive for permanent human presence in space are placing increasing demands on improvements in both space power generation and space thermal management capabilities. Efforts to develop lightweight space power generation capabilities in the megawatt to gigawatt range using a variety of technologies are in great demand. Power generation technologies being considered for space applications require the development or improvement of several subsystems that include solar photovoltaic cells, solar dynamic power modules, wireless transmission of power capabilities, integrated structure and power distribution systems, and space environmental damage control and safety enhancement capability, to name a few. These subsystems add to the overall system mass not only because of their inherent component mass, but also because of the increased mass of the thermal management system. For many space applications, of which space power generation is but one example, a lighter thermal management system is a strong driver in reducing the cost of the mission.

The classical design choice for thermal management is between passive systems, in which the radiator operates at a slightly lower temperature than the cooling load, and active systems, in which a heat pump drives the radiator to elevated temperatures. This paper analyzes a novel method for determining the viability of any space-operated thermally actuated heat pump with power and thermal management subsystems based on a single mass parameter. This system mass ratio (SMR) is a function of several key system parameters and was derived from fundamental thermodynamic analysis. System planners can use the SMR on a particular thermally actuated heat-rejection system to determine if a weight advantage exists over conventional methods currently in use. The SMR is based on a comparison of the overall system mass to the mass from an idealized passive radiator.

The purpose of this work is to determine the desirable regime of operation of such a power-refrigeration system for all potential space applications in terms of normalized temperatures as well as nondimensional structural and efficiency parameters. The SMR will be determined as a function of these temperature ratios at particular

values of the remaining parameters. This paper estimates the range of each parameter for a typical thermally actuated cooling system operating in space and creates a base model established from the state-of-the-art average values for each of the ranges. The overall effect that each parameter has on the SMR is demonstrated by increasing the variable in question by a certain percentage and examining the resulting change in the plotted curves. The results of this process will enable designers to make weight-saving decisions based on particular chosen values of each system parameter as well as provide a basis for optimization. Also, investigators can examine feasibility and ensure total system integration of the spacecraft/prime power system to many thermal suites while still in the conceptual stage.

To the authors' knowledge there does not exist a fundamental analysis for thermally actuated systems based solely on a weight parameter. This paper is an attempt to address the apparent need for such a design methodology for space applications. Many systems dealing with power and refrigeration management have been proposed for which this analysis can be used, including absorption heat systems and solar-powered vapor jet refrigeration systems. Examples of these systems are found in the works of Abrahamsson et al.,[1] Alefeld and Radermacher,[2] Anderson,[3] Chai and Lansing,[4] Chen,[5] and Lansing and Chai.[6]

However, this mass-based analysis was primarily motivated by a novel thermal management system termed the Solar Integrated Thermal Management and Power cycle (SITMAP) investigated by Nord et al.[7] This system essentially combines thermal management and a power-producing cycle into a single self-contained unit and can be powered entirely by solar thermal input. A jet pump serves as the compressor in the thermal management subsystem, reducing vibration and weight while increasing reliability. Examples of work relevant to the SITMAP investigation include Bredikhin et al.,[8] Cunningham and Dopkin,[9] Cunningham,[10] Elger et al.,[11] Fabri and Paulon,[12] Fabri and Siestrunk,[13] Fairuzov and Bredikhin,[14] Holladay and Hunt,[15] Holmes et al.,[16] Jiao et al.,[17] Lear et al.,[18] Marini et al.,[19] Neve,[20] and Sherif et al.[21]

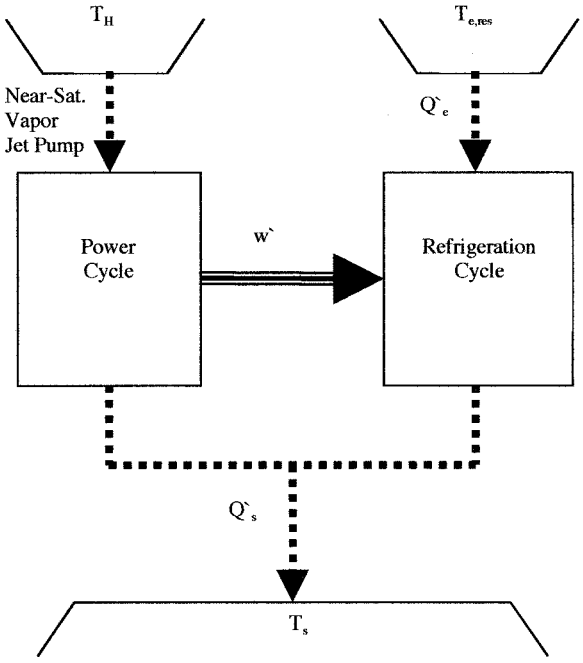

Fig. 1 Overall system schematic.

Analysis

System Definition

Figure 1 shows a schematic for the conceptual thermally actuated heat pump system being considered. The power subsystem accepts heat from a high-temperature source and supplies the power needed by the refrigeration subsystem. Both systems reject heat via a radiator to a common heat sink. The power cycle supplies just enough power internally to maintain and operate the refrigeration loop. However, in principle, the power cycle could provide power for other onboard systems if needed. Both the power and refrigeration systems are considered generic and can be modeled by any specific type of heat engine such as the Rankine, Sterling, and Brayton cycles for the power subsystem and gas refrigeration or vapor compression cycles for the cooling subsystem.

Figure 2 demonstrates how simple Rankine and vapor compression cycles can be used to model the power and cooling systems, respectively. A solar collector replaces the traditional boiler in the Rankine cycle, and the condenser is replaced by a common radiator to approximate potential applications operating in space. However, this analysis is not limited to these basic heat engine systems. They are shown only for ease of reference to the fluid stream temperatures.

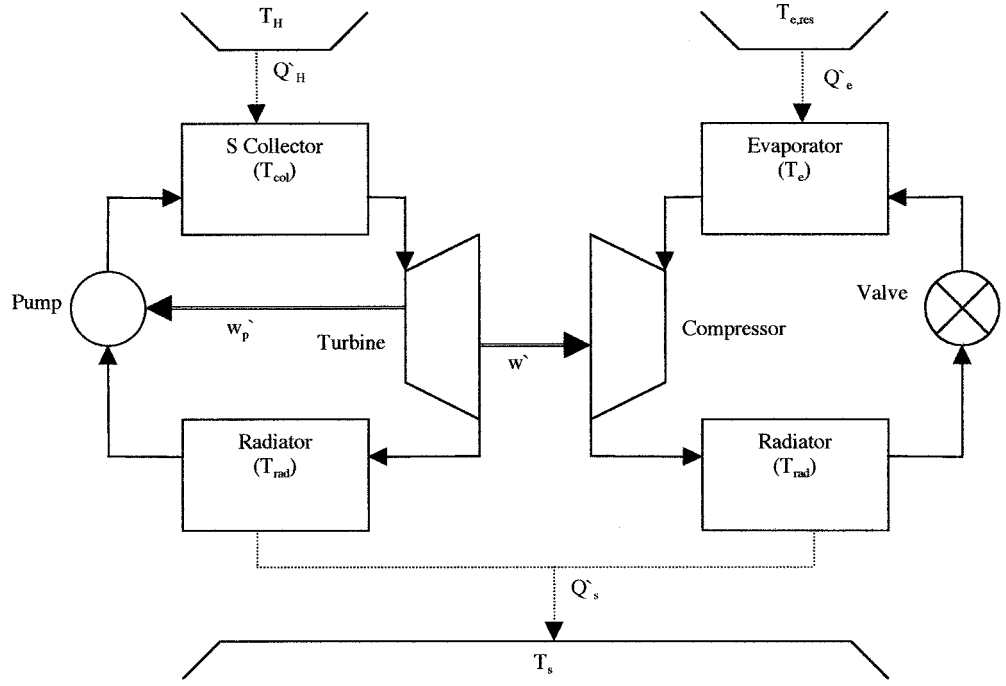

Fig. 2 Overall system with Rankine and vapor compression cycles representing the power and refrigeration cycles, respectively.

SMR Definition

Heat pumps like those demonstrated in Figs. 1 and 2 involve system complexity that passive systems do not have. Therefore, to justify their use for space applications, a significant reduction of the overall system mass must be present. It is for this reason that an analysis was undertaken to derive a single mass parameter as a figure-of-merit. The SMR is defined as the total system mass normalized to the mass of an idealized passive system. This is shown mathematically by

$$\tilde{m} = \frac{m_{\text{col}} + m_{\text{rad}} + m_{\text{sys}}}{m_{\text{rad,o}}} \tag{1}$$

This equation can be separated and rewritten in terms of collector and radiator areas

$$\tilde{m} = \frac{(\lambda_{\text{col}}/\lambda_{\text{rad}})A_{\text{col}} + A_{\text{rad}}}{A_{\text{rad,o}}} + \frac{m_{\text{sys}}}{m_{\text{rad,o}}} \tag{2}$$

The total system mass is divided into three terms for ease of manipulation. The last mass term m_{sys} represents the mass of the turbomachinery and piping present in an active system. Also, notice that λ is defined in units of mass per area rather than the more familiar density, which has units of mass per volume.

Solar Collector Model

The solar collector was modeled by examining the solar energy incident on its surface. This energy is proportional to the collector efficiency, the cross-sectional area that is absorbing the flux, and the local radiant solar heat flux G_{sun}. This is shown by

$$Q'_H = \eta_{\text{col}} G_{\text{sun}} A_{\text{col}} \tag{3}$$

Radiator Model

The radiant energy transfer rate between the radiator and the environment is given next. For deep space applications the environmental reservoir temperature might be neglected, but for near-planetary or solar missions this might not be the case.

$$Q'_s = \varepsilon\sigma A_{\text{rad}}\left(T_{\text{rad}}^4 - T_s^4\right) \tag{4}$$

In the idealized passive radiator model, $\varepsilon = 1$, and the entire surface of the radiator is at the same temperature as the evaporator. Because there is no additional thermal input, the heat transferred to the radiator is equal to that from the evaporator. The ideal passive area for a radiator is consistent with

$$Q'_{\text{passive}} = \sigma A_{\text{rad,o}}\left(T_e^4 - T_s^4\right) = Q'_e \tag{5}$$

Overall System Analysis

Solving Eqs. (3–5) for the collector and the radiator areas and substituting into the first term of Eq. (2) yields

$$\tilde{m} = \left[\alpha\frac{Q'_H}{\eta_{\text{col}} G_{\text{sun}}} + \frac{Q'_s}{\varepsilon\sigma\left(T_{\text{rad}}^4 - T_s^4\right)}\right] \Bigg/ \frac{Q'_e}{\sigma\left(T_e^4 - T_s^4\right)} + \frac{m_{\text{sys}}}{m_{\text{rad,o}}} \tag{6}$$

A new nondimensional term α is introduced in Eq. (7) to further simplify the system mass ratio:

$$\alpha = \lambda_{\text{col}}/\lambda_{\text{rad}} \tag{7}$$

Next an overall energy balance is performed on the active system so that the heat transfer rate from the radiator can be expressed in an alternative form:

$$Q'_H + Q'_e = Q'_s \tag{8}$$

Equation (8) is substituted into Eq. (6) to obtain

$$\tilde{m} = \left[\alpha\frac{Q'_H}{\eta_{\text{col}} G_{\text{sun}}} + \frac{Q'_e + Q'_H}{\varepsilon\sigma\left(T_{\text{rad}}^4 - T_s^4\right)}\right] \Bigg/ \frac{Q'_e}{\sigma\left(T_e^4 - T_s^4\right)} + \frac{m_{\text{sys}}}{m_{\text{rad,o}}} \tag{9}$$

which can be expanded to

$$\tilde{m} = \frac{1}{\varepsilon}\left\{\frac{Q'_H}{Q'_e}\left(1 - \left(\frac{T_s}{T_e}\right)^4\right)\left[\frac{\alpha\varepsilon\sigma T_e^4}{\eta_{\text{col}} G_{\text{sun}}} + \left(\frac{T_e}{T_{\text{rad}}}\right)^4\left(\frac{1}{1 - (T_s/T_{\text{rad}})^4}\right)\right] + \left(\frac{T_e}{T_{\text{rad}}}\right)^4\left(\frac{1 - (T_s/T_e)^4}{1 - (T_s/T_{\text{rad}})^4}\right)\right\} + \frac{m_{\text{sys}}}{m_{\text{rad,o}}} \tag{10}$$

The thermal efficiency and the coefficient of performance for the power and refrigeration cycles are now introduced into the analysis. These quantities can be related because the work output from the power cycle is equal to the work input for the refrigeration cycle according to the active system model.

$$\eta = w'/Q'_H \tag{11}$$

$$\text{COP} = Q'_e/w' \tag{12}$$

Solving for w' in Eq. (11) and substituting into Eq. (12) allows the coefficient of performance and thermal efficiency to be expressed as a ratio of heat rates:

$$\eta\text{COP} = Q'_e/Q'_H \tag{13}$$

Next, Eq. (13) is substituted into Eq. (10) and further simplified as shown:

$$\tilde{m} = \frac{1}{\varepsilon}\left\{\frac{\left[1 - (T_s/T_e)^4\right]}{\eta\text{COP}}\left[\frac{\alpha\varepsilon\sigma_e T_e^4}{\eta_{\text{col}} G_{\text{sun}}} + \left(\frac{T_e}{T_{\text{rad}}}\right)^4\left(\frac{1}{1 - (T_s/T_{\text{rad}})^4}\right)\right] + \left(\frac{T_e}{T_{\text{rad}}}\right)^4\left(\frac{1 - (T_s/T_e)^4}{1 - (T_s/T_{\text{rad}})^4}\right)\right\} + \frac{m_{\text{sys}}}{m_{\text{rad,o}}} \tag{14}$$

It is now necessary to relate the COP and the thermal efficiency to the fluid temperatures of the radiator and the collector. To do this, a relationship must be established between the limiting Carnot cases for both parameters. With good design some fraction of the Carnot limits is expected for the power and thermal subsystems. This fraction or percentage of Carnot would also be a good indicator of the system technology level. Therefore, two new system parameters are defined so that the thermal efficiency and the COP do not exceed the Carnot limits.

$$\xi_P = \eta/\eta_C \tag{15}$$

$$\xi_R = \text{COP}/\text{COP}_C \tag{16}$$

It follows that the thermal efficiency of a Carnot direct heat engine is described by

$$\eta_C = 1 - (T_{\text{rad}}/T_{\text{col}}) \tag{17}$$

Similarly, it is readily shown that the coefficient of performance for a Carnot refrigerator or air conditioner is described by

$$\text{COP}_C = T_e/(T_{\text{rad}} - T_e) \tag{18}$$

Substituting Eqs. (15–18) into Eq. (14) and simplifying produces the following:

$$\tilde{m} = \frac{1}{\varepsilon}\left[\frac{\left[1 - (T_s/T_e)^4\right]}{\xi_P\xi_R(1 - T_{\text{rad}}/T_{\text{col}})[T_e/(T_{\text{rad}} - T_e)]}\left(\frac{\alpha\varepsilon\sigma T_e^4}{\eta_{\text{col}} G_{\text{sun}}} + \left(\frac{T_e}{T_{\text{rad}}}\right)^4\left\{\frac{1}{1 - [(T_s/T_e)(T_e/T_{\text{rad}})]^4}\right\}\right) + \left(\frac{T_e}{T_{\text{rad}}}\right)^4\left[\frac{1 - (T_s/T_e)^4}{1 - (T_s/T_{\text{rad}})^4}\right]\right] + \frac{m_{\text{sys}}}{m_{\text{rad,o}}} \tag{19}$$

Next, all temperature ratios shown in Eq. (19) are normalized to the fluid evaporator temperature. This results in three new nondimensional temperature ratios being defined and allows the SMR to be determined as a function of these ratios later on.

$$T^*_{\text{col}} = T_{\text{col}}/T_e \tag{20}$$

$$T^*_{\text{rad}} = T_{\text{rad}}/T_e \tag{21}$$

$$T^*_s = T_s/T_e \tag{22}$$

These terms are introduced into Eq. (19) to give

$$\tilde{m} = \frac{1}{\varepsilon}\left\{\frac{T^*_{\text{col}}\left(T^*_{\text{rad}}-1\right)\left(1-T^{*4}_s\right)}{\xi_P\xi_R\left(T^*_{\text{col}}-T^*_{\text{rad}}\right)}\left[\frac{\alpha K_e T_e^4}{K_H}+\left(\frac{1}{T^{*4}_{\text{rad}}-T^{*4}_s}\right)\right]+\left(\frac{1-T^{*4}_s}{T^{*4}_{\text{rad}}-T^{*4}_s}\right)\right\}+\frac{m_{\text{sys}}}{m_{\text{rad,o}}} \tag{23}$$

where K_e and K_H are introduced for convenience to group constants.

Two more nondimensional parameters are defined: the first represents a dimensionless structural parameter, which is a strong function of the evaporator temperature, and the second is the product of the two fractions of the Carnot parameters introduced in Eqs. (15) and (16).

$$\zeta = \frac{\alpha\varepsilon\sigma T_e^4}{\eta_{\text{col}} G_{\text{sun}}} \tag{24}$$

$$\xi_T = \xi_P\xi_R \tag{25}$$

Therefore, Eq. (23) can again be rewritten as follows:

$$\tilde{m} = \frac{1}{\varepsilon}\left\{\frac{T^*_{\text{col}}\left(T^*_{\text{rad}}-1\right)\left(1-T^{*4}_s\right)}{\xi_T\left(T^*_{\text{col}}-T^*_{\text{rad}}\right)}\left[\zeta+\left(\frac{1}{T^{*4}_{\text{rad}}-T^{*4}_s}\right)\right]+\left(\frac{1-T^{*4}_s}{T^{*4}_{\text{rad}}-T^{*4}_s}\right)\right\}+\frac{m_{\text{sys}}}{m_{\text{rad,o}}} \tag{26}$$

The second term in Eq. (26) will now be considered. Applying dimensional analysis to the third term on the right-hand side yields

$$(m_{\text{sys}}/m_{\text{t,act}})(m_{\text{t,act}}/m_{\text{rad,o}}) = (m_{\text{sys}}/m_{\text{t,act}})\tilde{m} \tag{27}$$

The additional mass term $m_{\text{t,act}}$ represents the total mass of the system being analyzed and is defined in terms of the other mass parameters by the following:

$$m_{\text{t,act}} = m_{\text{rad}} + m_{\text{col}} + m_{\text{sys}} \tag{28}$$

Substituting Eq. (27) into Eq. (26), the latter can be written as

$$\tilde{m} = \frac{1}{\varepsilon}\left\{\frac{T^*_{\text{col}}\left(T^*_{\text{rad}}-1\right)\left(1-T^{*4}_s\right)}{\xi_T\left(T^*_{\text{col}}-T^*_{\text{rad}}\right)}\left[\zeta+\left(\frac{1}{T^{*4}_{\text{rad}}-T^{*4}_s}\right)\right]+\left(\frac{1-T^{*4}_s}{T^{*4}_{\text{rad}}-T^{*4}_s}\right)\right\}+\frac{m_{\text{sys}}}{m_{\text{t,act}}}\tilde{m} \tag{29}$$

Another nondimensional system parameter is defined next. This parameter indicates the percentage of mass that the piping and turbomachinery contribute to the overall system mass:

$$\mu = m_{\text{sys}}/m_{\text{t,act}} \tag{30}$$

Substituting this mass parameter into Eq. (29), the general form of the SMR for an active system is obtained:

$$\tilde{m} = \frac{1}{\varepsilon(1-\mu)}\left\{\frac{T^*_{\text{col}}\left(T^*_{\text{rad}}-1\right)\left(1-T^{*4}_s\right)}{\xi_T\left(T^*_{\text{col}}-T^*_{\text{rad}}\right)}\left[\zeta+\left(\frac{1}{T^{*4}_{\text{rad}}-T^{*4}_s}\right)\right]+\left(\frac{1-T^{*4}_s}{T^{*4}_{\text{rad}}-T^{*4}_s}\right)\right\} \tag{31}$$

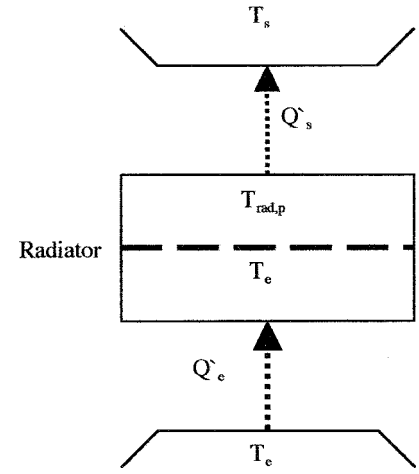

Fig. 3 Schematic of an actual passive radiator system.

Equation (31) represents the SMR in terms of seven system parameters. Three of these parameters are based on temperature ratios, and the remaining four are based on system properties. All of the parameters are quantities that can be computed for a given application.

Deep Space Applications

For applications where the load temperature can be approximated as zero Kelvin (deep space), the equation for the SMR reduces to the following:

$$\tilde{m} = \left\{\frac{T^*_{\text{col}}\left(T^*_{\text{rad}}-1\right)}{\xi_T\left(T^*_{\text{col}}-T^*_{\text{rad}}\right)}\left[\zeta+\left(\frac{1}{T^*_{\text{rad}}}\right)^4\right]+\left(\frac{1}{T^*_{\text{rad}}}\right)^4\right\}\Big/\left[\varepsilon(1-\mu)\right] \tag{32}$$

Realistic Passive Radiator Model Comparison

The figure of merit is based on the ratio between the mass of the total system to the mass of an ideal passive radiator. The derived equation has a limiting value of unity below which the value of the SMR for a particular application cannot descend. However, the values of the SMR for different systems can be compared to each other. In particular, it is desirable if a comparison can be made to a realistic passive radiator where there is temperature drop between the inlet and outlet and the emissivity is not equal to unity. This comparison will demonstrate whether a weight benefit exists over conventional passive methods. A general schematic for an actual passive radiator operating at the reservoir source temperature T_e is shown below.

A similar mass-based analysis was performed on this system. The result is given by

$$\tilde{m} = [1/\varepsilon(1-\mu)]\left[\left(1-T^{*4}_s\right)\Big/\left(T^{*4}_{\text{rad,p}}-T^{*4}_s\right)\right] \tag{33}$$

The additional temperature term $T^*_{\text{rad,p}}$ represents the ratio between the actual passive radiator temperature and the temperature of the high temperature source such that

$$T^*_{\text{rad,p}} = T_{\text{rad,p}}/T_e \tag{34}$$

For a given application of an active space-operated system, two different mass parameters need to be computed; one for the active system given by Eq. (31) and one for the actual passive radiator given by Eq. (33). If the SMR for the active system falls below that for the passive case, the active system under consideration is a viable option based on the overall reduction of system mass.

Results and Discussion

The system mass ratio given by Eq. (31) is a function of three temperature ratios (one environmental, two system) and four structural parameters. Estimating a range for each parameter and taking an

overall average for all parameters, a base comparison case was created. The effect of each individual parameter can be demonstrated by simply changing the parameter in question by around 20% while maintaining all other parameters at their base value. For a given application the five structural and environmental variables will be determined from subsystem design considerations, and the remaining two system temperature ratios can be optimized to obtain the lowest possible SMR. However, because the analysis is intended to be universal in nature it is useful to vary each parameter in question to illustrate all potential areas of application. An optimization analysis can be performed on any active system once the structural and environmental parameters are determined for the system. Technology projections can also be performed to determine crossover points where active systems should be considered.

The range of the five structural and environmental parameters is discussed next, beginning with the emissivity. A conservative range of 0.78–0.95 was assumed, and an average value of 0.865 was used in the base model for emissivity. The parameter ξ_T, given by Eq. (25), indicates the product of the two fractional percentages of Carnot for the refrigeration and power cycles. The parameter was estimated to range from 0.1 for a highly inefficient system to 0.5 for a moderately efficient system. The average ξ_T used for the base model was 0.3. The structural parameter μ is estimated to be around 0.5 for the base condition. This value was derived by estimating that the mass of the piping and turbomachinery accounts for nearly half of the overall weight of an active system. The environmental parameter T_s^* given by Eq. (22) was assumed to be zero for the base model comparison. This would accurately model conditions where a deep space thermally actuated system might operate, where the sink temperature is approximated as zero Kelvin. However, for applications where a system may be operating in low Earth orbit the surrounding sink temperature might be around $-60°$C. This temperature would make the nondimensional temperature term T_s^* equal to around 0.7 if the evaporator temperature, by which all temperatures are normalized, is assumed to range from 300–325 K.

The parameter ζ given by Eq. (24) is itself a function of four variables. Each of these variables has a range and an average assumed value. The maximum value of ζ was obtained by combining the highest possible combination of the four variables, and the minimum value was similarly obtained by using the lowest combination for each range of the variables. The range of each of these variables is discussed briefly next. The term α given by Eq. (7) indicates the mass/area ratio of the collector to that of the radiator. The state-of-the-art collector is estimated to be around 0.2 kg/m^2, and the current collectors can be around 2 kg/m^2. An average value of 6 kg/m^2 was used for the radiator. Therefore α has a numerical range from 0.033 to 0.333 and a base value of 0.18. The temperature of the evaporator was already discussed, and the efficiency of the collector is estimated to vary from 0.6 to 0.8. Using these ranges, a maximum value of 0.246 was obtained for ζ. The corresponding minimum and base values for ζ are 0.011 and 0.129, respectively.

The actual passive model comparison given by Eq. (33) is also a function of four independent parameters. Three of these parameters also appear in Eq. (31) for the general system analysis. However, it is important to note that these parameters are not directly related to each other. That is, the range that applies to the parameters for the active system's SMR is not necessarily the same as that in the realistic passive model. The emissivity is assumed to have a slightly higher and more restricted range of 0.90–0.95. The system mass term μ is assumed to vary from 0.3 to 0.5. The environmental temperature term T_s^* is assumed to vary from 0 to 0.7. The last term $T_{\text{rad,p}}^*$ indicates the temperature drop across a realistic passive radiator. The drop is estimated around 10%, which gives a range of around 0.9 to 0.95 for the nondimensional parameter $T_{\text{rad,p}}^*$.

By definition, the SMR for any real system cannot be smaller than that for the ideal case, which is unity for an ideal passive radiator operating perfectly with no additional system mass as a result of piping. However, by applying the appropriate ranges just discussed for actual passive systems a region can be determined for which the active system in question can be considered viable. In Figs. 4–9 a gray shaded area indicates an approximate zone in which a realistic radiator might operate. If the SMR for the active system in question falls in or below this region, the active system will have a weight advantage over conventional passive systems.

Figure 4 displays the base case in which the SMR is plotted as a function of collector temperatures for specific values of radiator temperature. All system parameters have values at the average of each of their respective ranges. The range for the radiator temperature ratio was chosen to model most accurately a typical thermally actuated system where the radiator temperature is at most double the evaporator temperature. For a particular value of collector temperature, there is observed to be a single radiator temperature that will minimize the SMR. Also, if the SMR lies within the shaded actual passive system region, there might be a reduction of overall system mass when compared to more traditional passive systems. Of course, if the value of the SMR lies below this passive region there is a compelling mass savings advantage for the active system.

Figure 5 demonstrates the effect of increasing T_s^* on the SMR. Increasing the environmental temperature ratio to model situations where active systems might be operating in low Earth orbit shifts

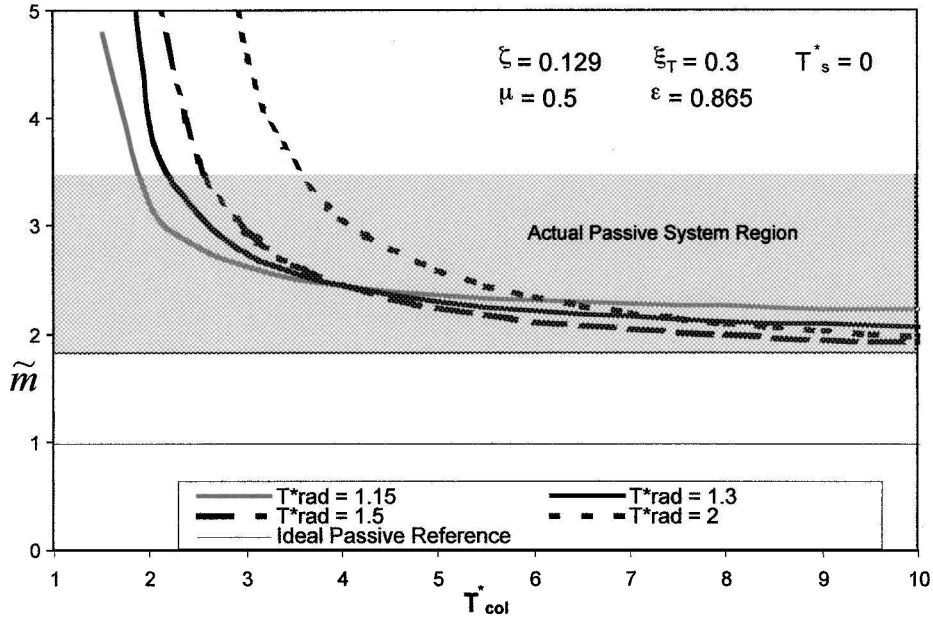

Fig. 4 Variation of the system mass ratio (SMR) as a function of normalized collector temperature: base model.

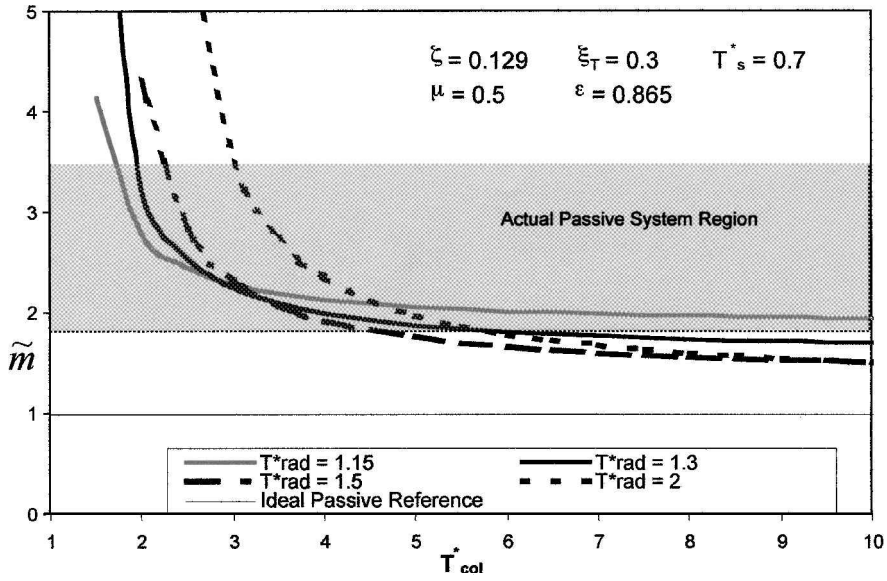

Fig. 5 Variation of the SMR as a function of normalized collector temperature: Effect of T_s^* is shown by increasing its base value to 0.7.

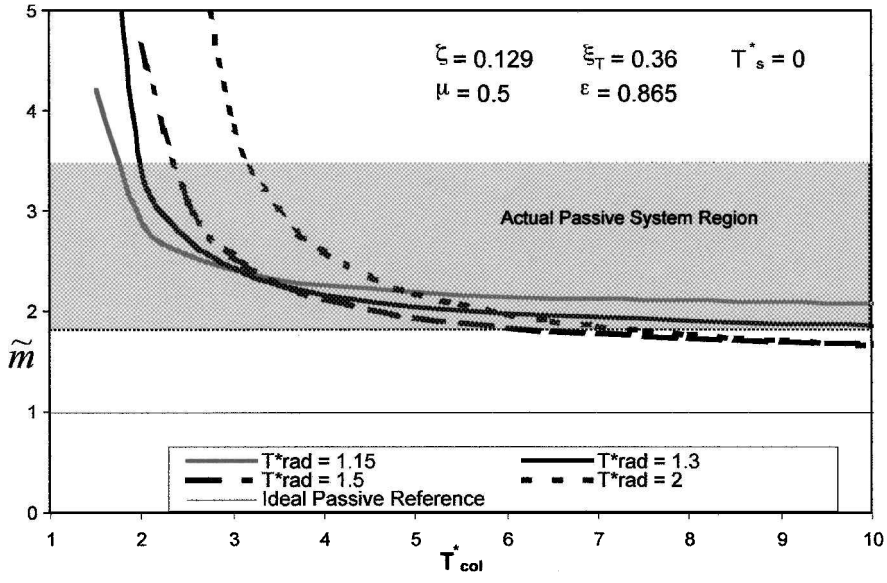

Fig. 6 Variation of the SMR as a function of normalized collector temperature: Effect of ξ_T is shown by increasing its base value by 20%.

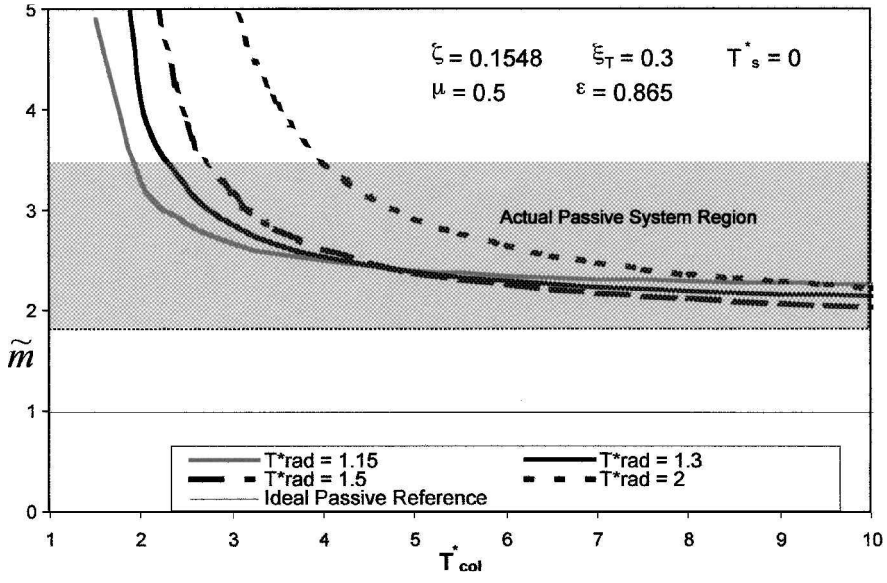

Fig. 7 Variation of the SMR as a function of normalized collector temperature: Effect of ζ is shown by increasing its base value by 20%.

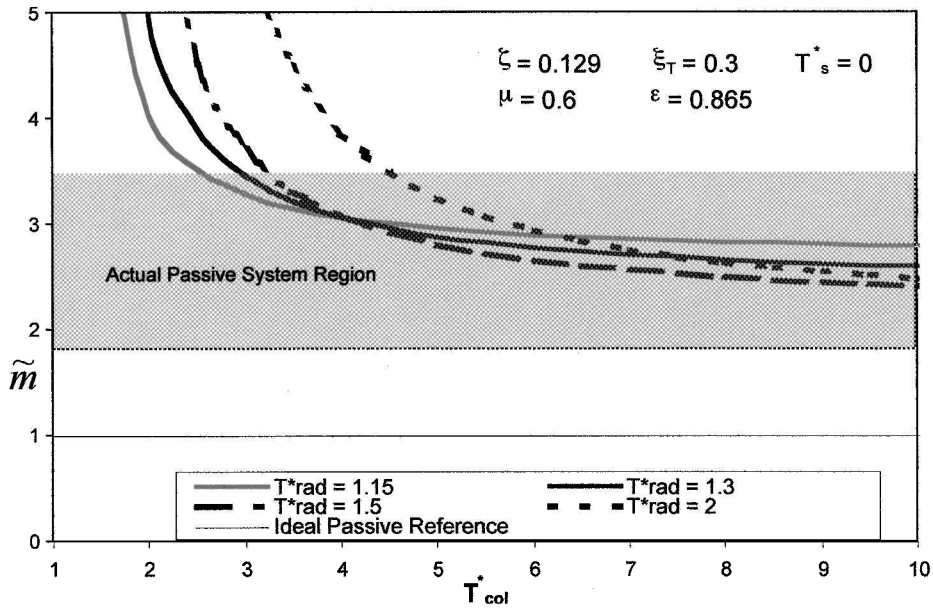

Fig. 8 Variation of the SMR as a function of normalized collector temperature: Effect of μ is shown by increasing its base value by 20%.

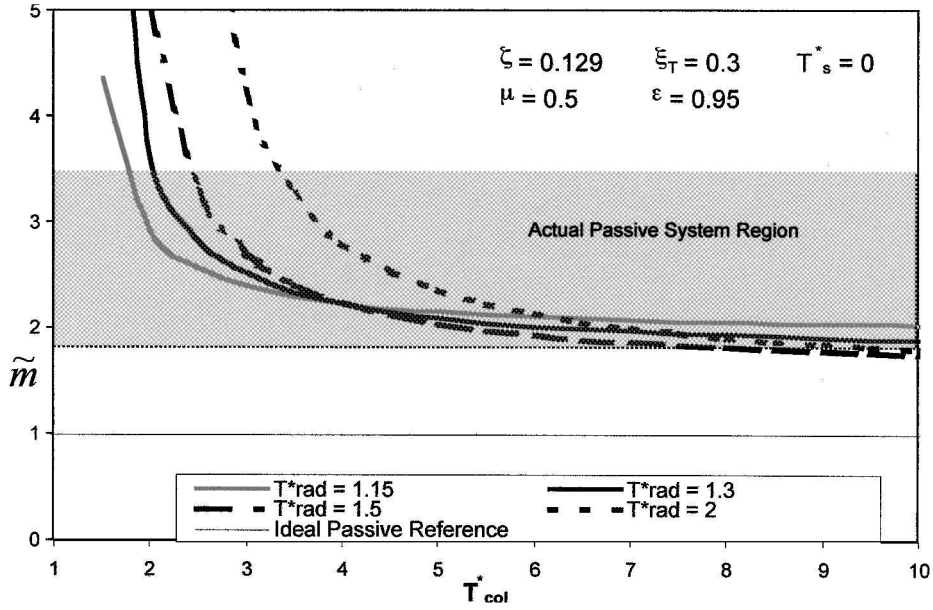

Fig. 9 Variation of the SMR as a function of normalized collector temperature: Effect of ε is shown by increasing its base value by 20%.

the family of curves downward and thus increases the mass savings achievable with an active system. The values for the SMR also fall below the shaded region for large values of collector temperature, which indicates an absolute mass weight advantage over traditional passive systems. The overall trends and shape of the curves remain the same as for the base case.

Figure 6 displays the result of increasing the product of the two Carnot parameters by 20%. As predicted, a slight increase in the Carnot parameters results in a considerable downward shift for the family of curves from the base case. Systems that are highly efficient might be able to achieve considerable weight savings for particular values of temperature ratios. Likewise, inefficient systems might have a more difficult task of proving an advantage over conventional passive systems, based solely on a mass parameter.

Figure 7 demonstrates the adverse effect of increasing ζ by 20%. The parameter ζ is a function of four parameters, but is most influenced by changes in α (collector mass/area ratio per radiator mass/area ratio). This variable has the greatest range of the four parameters based on the wide range of solar collector technology. When a state-of-the-art collector is used, α is decreased by a factor of two, which also decreases ζ by the same amount. The parameter ζ is also highly dependent on the evaporator fluid temperature. Therefore, lower values of evaporator temperature result in shifting the family of curves downward and thus decrease the values of the SMR. The parameter ζ has a weak dependence on emissivity and the collector efficiency. Clearly, lightweight systems and low evaporator temperatures favor active systems.

Figure 8 demonstrates that higher values of μ will have an adverse effect on the values of the SMR. This is expected because increasing μ physically relates to adding system mass, probably through piping and turbomachinery. Obviously, as more mass is added to the system the SMR will increase. Figure 9 shows that the radiator emissivity has only a marginal benefit on the values of the SMR. Increasing emissivity by around 20% shifts the family of curves downward but not significantly. SMR appears to have a weaker dependence on emissivity than the other parameters.

The system mass ratio is highly dependent on the temperature ratios for the radiator and collector, as shown in Figs. 4–9. For a particular space application the environmental and system parameters, which were estimated in order to construct the figures, will be

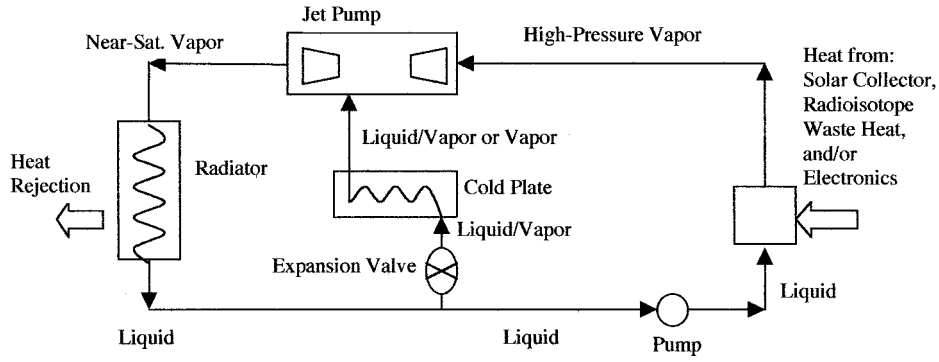

Fig. 10 Schematic of a thermally driven heat pump.

prescribed values. The fluid temperatures of the solar collector and radiator can then be set so as to optimize the mass savings based on Eq. (31). It is observed that for a given value of T_{col} there exits a value of T_{rad} that will optimize the SMR.

Examples

Previous work by the authors[7,18,21] identified some new developments in the fundamentals of compressible flow two-phase jet pumps. Previously, jet pumps of this nature were not well understood. The capability now exists to perform design and optimization as a result of this work. We propose three concepts to take advantage of these new developments.

Concept 1: Jet Pump System

As shown in Fig. 10, the technique is to raise the temperature of the heat-rejection radiator, thereby lowering the required radiator area. Less area means less mass. Past schemes to achieve a higher radiator temperature have called for a vapor compression pump with a reciprocating piston or rotor. Vibration and required input power are a problem for these systems. These have generally not made the weight trade because these devices and associated control electronics add more weight than the higher temperature radiator saves. Also, the electricity required to power the vapor compression pump means more mass in terms of a larger solar array and other spacecraft power management and distribution components. Our proposed system needs a high-temperature source of heat to drive the thermal system. This could be waste heat, a solar concentrator, or even a flat-plat solar collector, depending on the load temperature. For some low-temperature applications no solar input is needed; instead, waste heat from room-temperature electronics will drive the cycle.

The idea here is to use a jet pump instead of a vapor compression pump. A jet pump is a pair of concentric tubes, in which usually the center tube consists of a nozzle of a high-pressure jet of fluid. The jet action creates a low-pressure suction at the nozzle opening. The jet pump has been used in large industrial air conditioning systems, primarily with the working fluid being steam. The jet pump weighs very little because it is basically a pair of concentric tubes. One issue is that the appropriate system temperature range is highly dependent on the choice of working fluid. However, two example concepts are presented later, which show concrete evidence of potentially real mission advantages. Another issue is the lower component efficiency of the jet pump as compared to a rotating or reciprocating vapor compressor. However, this should be traded against the mass, cost, and no-moving-parts advantages. A methodology for quickly assessing these trades has been developed and is currently being investigated by the authors as part of a NASA-sponsored research program.

Concept 2: Jet Pump/Electrically Driven Mechanical Pump

Flight qualified, long-life single-phase liquid pumps have flown on spacecraft in the past, such as the successful Mars Pathfinder, and will fly on spacecraft in the future, such as the International Space Station. These pumps require spacecraft electrical power. However, the thermodynamics is such that the electrical power required to affect the pressure difference is only a tiny fraction of that needed for the more familiar vapor compression pump. The scheme essentially retains the advantages of the thermal pump in that energy to drive the system basically comes from the solar collector or waste heat sources.

Concept 3: Jet Pump/Mechanical Pump/Turbine

For very large systems, such as those proposed for the Space Solar Power Project, a rotating turbine can be added to the system to generate power via a Rankine cycle loop. Rankine and other power cycles have been studied extensively for high-power spacecraft. Recent interest in the Space Solar Power concept requires that these technologies be investigated in light of new developments in new analysis capabilities and flight experience. Combining the thermal management and power generation within one system can make the weight trade against conventional solar cells, which have been used since the dawn of the space age. Our analysis is not restricted to the Rankine cycle, but also applies to the Stirling and other power cycles, the optimal choice depending on the particular design constraints.

Conclusions

This paper has described a parametric analysis leading to a single mass-based parameter for any thermally actuated heat pump operating in space. With the use of this mass parameter, a comparison between active and passive systems was made to determine conditions under which active systems possess an advantage based on mass savings over their passive counterparts. The conditions were determined by examining the effect of each temperature ratio and system parameter on the mass-based figure of merit. The following conclusions were drawn regarding these dependencies based on this study:

1) Active systems should be considered, in order to minimize weight, when low evaporator fluid temperatures are desired.

2) Active systems should be considered, in order to minimize weight, when the collector fluid temperature is at least three or four times greater than the evaporator fluid temperature.

3) The overall mass advantage for active systems increases as the environmental sink temperature is increased, for constant values of all other parameters.

4) System mass decreases rapidly with respect to the efficiency ξ_T of both the refrigeration and power cycles.

5) The overall mass of active systems decreases by minimizing the structural parameter ζ. This parameter is most sensitive to solar collector technology and the evaporator fluid temperature. Higher collector efficiency and radiator emissivity also directly influence this parameter.

6) Decreasing the weight of piping and turbomachinery will also reduce the value of the system mass ratio and thus reduce the overall system mass.

7) For specific values of each system parameter and collector fluid temperature, there exists a radiator fluid temperature that will optimize the mass savings for an active system.

It follows from the preceding conclusions that, for the configuration and ranges studied, particular active systems can in fact have a significant reduction of mass over more conventional passive systems. Currently, the mass-based parameter, SMR, is being applied

to the SITMAP cycle, discussed in the Introduction section, to determine the viability of such a system based on weight and economic savings.

Acknowledgments

The authors are indebted to the support provided by Jim Nord of Rocketdyne. Support from the Department of Mechanical and Aerospace Engineering at the University of Florida is also gratefully acknowledged.

References

[1]Abrahamsson, K., Jernqvist, A., and Ally, G., "Thermodynamic Analysis of Absorption Heat Cycles," *Proceedings of the International Absorption Heat Pump Conference*, AES-Vol. 31, American Society of Mechanical Engineers, New York, 1994, pp. 375–383.

[2]Alefeld, G., and Radermacher, R., *Heat Conversion Systems*, CRC Press, Boca Raton, FL, 1994.

[3]Anderson, H., "Assessment of Solar Powered Vapor Jet Air-Conditioning System," *International Solar Energy Congress and Exposition (ISES)*, International Solar Energy Society, Freiburg, Germany, 1975, p. 408.

[4]Chai, V. W., and Lansing, F. L., "A Thermodynamic Analysis of a Solar-Powered Jet Refrigeration System," Jet Propulsion Lab., California Inst. of Technology, DSN Progress Rept. 41-42, Pasadena, CA, 1977, pp. 209–217.

[5]Chen, L. T., "Solar Powered Vapor-Compressive Refrigeration System Using Ejector as the Thermal Compressors," *Proceedings of the National Science Council*, Pt. 3, No. 10, 1977, pp. 115–132.

[6]Lansing, F. L., and Chai, V. W., "Performance of Solar-Powered Vapor-Jet Refrigeration Systems with Selected Working Fluids," Jet Propulsion Lab., California Inst. of Technology, DSN Progress Rept. 42-44, Pasadena, CA, 1978, pp. 245–248.

[7]Nord, J. W., Lear, W. E., and Sherif, S. A., "Design Analysis of a Heat-Driven Jet Pumped Cooling System for Space Thermal Management Applications," *Journal of Propulsion and Power*, Vol. 17, No. 3, 2001, pp. 566–570.

[8]Bredikhin, V. V., Gorbenko, G. A., Nikonov, A. A., and Fairuzov, Y. V., "Mathematical Modeling of Thermo-Circulating Loops with Jet Pumps," *Hydrodynamic Processes in Multi-Phase Working Fluid Energy Plants*, Kharkov Aviation Inst., Kharkov, Ukraine, 1990, pp. 3–10 (in Russian).

[9]Cunningham, R. G., and Dopkin, R. J., "Jet Breakup and the Mixing Throat Lengths for the Liquid Jet Pump," *Journal of Fluids Engineering*, Vol. 96, No. 3, 1974, pp. 216–226.

[10]Cunningham, R. G., "Liquid Jet Pumps for Two-Phase Flows," *Journal of Fluids Engineering*, Vol. 117, No. 2, 1995, pp. 309–316.

[11]Elger, D. F., McLam, E. T., and Taylor, S. J., "A New Way to Represent Jet Pump Performance," *Journal of Fluids Engineering*, Vol. 113, No. 3, 1991, pp. 439–444.

[12]Fabri, J., and Paulon, J., "Theory and Experiments on Air-to-Air Supersonic Ejectors," NACA-TM-1410, Sept. 1958.

[13]Fabri, J., and Siestrunk, R., "Supersonic Air Ejectors," *Advances in Applied Mechanics*, edited by H. L. Dryden and Th. von Karman, Vol. V, Academic Press, New York, 1958, pp. 1–33.

[14]Fairuzov, Y. V., and Bredikhin, V. V., "Two Phase Cooling System with a Jet Pump for Spacecraft," *Journal of Thermophysics and Heat Transfer*, Vol. 9, No. 2, 1995, pp. 285–291.

[15]Holladay, J. B., and Hunt, P. L., "Fabrication, Testing, and Analysis of a Flow Boiling Test Facility with Jet Pump and Enhanced Surface Capability," NASA Marshall Space Flight Center, Thermal and Life Support Division, Research Proposal, Huntsville, AL, Jan. 1996.

[16]Holmes, H. R., Geopp, J., and Hewitt, H. W., "Development of the Lockheed Pumped Two Phase Thermal Bus," AIAA Paper 87-1626, June 1987.

[17]Jiao, B., Blais, R. N., and Schmidt, Z., "Efficiency and Pressure Recovery in Hydraulic Jet Pumping of Two-Phase Gas/Liquid Mixtures," *SPE Production Engineering*, Vol. 5, No. 4, 1990, pp. 361–364.

[18]Lear, W. E., Sherif, S. A., Steadham, J. M., Hunt, P. L., and Holladay, J. B., "Design Considerations of Jet Pumps with Supersonic Two-Phase Flow and Shocks," AIAA Paper 99-0461, Jan. 1999.

[19]Marini, M., Massardo, A., Satta, A., and Geraci, M., "Low Area Ratio Aircraft Fuel Jet-Pump Performance with and Without Cavitation," *Journal of Fluids Engineering*, Vol. 114, No. 4, 1992, pp. 626–631.

[20]Neve, R. S., "Diffuser Performance in Two-Phase Jet Pump," *International Journal of Multiphase Flow*, Vol. 17, No. 2, 1991, pp. 267–272.

[21]Sherif, S. A., Lear, W. E., Steadham, J. M., Hunt, P. L., and Holladay, J. B., "Analysis and Modeling of a Two-Phase Jet Pump of a Thermal Management System for Aerospace Applications," *International Journal of Mechanical Sciences*, Vol. 42, No. 2, 2000, pp. 185–198.